

First-principles dynamical CPA to finite-temperature magnetism of transition metals¹

Y Kakehashi, T Tamashiro, M A R Patoary, and T Nakamura

University of the Ryukyus, Nishihara, Okinawa, Japan

E-mail: yok@sci.u-ryukyu.ac.jp

Abstract. We present here the first-principles dynamical CPA (coherent potential approximation) combined with the tight-binding LMTO LDA+U method towards quantitative calculations of the electronic structure and magnetism at finite temperatures in transition metals and compounds. The theory takes into account the single-site dynamical charge and spin fluctuations using the functional integral technique as well as an effective medium. Numerical results for Fe, Co, and Ni show that the theory explains quantitatively the high-temperature properties such as the effective Bohr magneton numbers and the excitation spectra in the paramagnetic state, and describes the Curie temperatures semiquantitatively.

Quantitative description of the magnetic properties of materials has been one of the goals in magnetism. For the ground-state properties of transition metals and alloys, such a calculation scheme has been realized by the density functional theory (DFT). The DFT quantitatively explains the ground-state magnetizations of Fe, Co, and Ni as well as their cohesive properties. At finite temperatures, on the other hand, it does not explain the local-moment behavior such as the Curie-Weiss susceptibilities, and overestimates the Curie temperature by a factor of ten due to neglect of the spin fluctuations. Because of these difficulties, quantitative description of the finite temperature magnetism has been a long-standing problem in the metallic magnetism [1].

Quite recently, we have proposed the dynamical coherent potential approximation (CPA) [2] combined with the first-principles tight-binding (TB) linear muffin-tin orbital (LMTO) method [3] with LDA(Local Density Approximation)+U potential [4] for band calculations, and presented the numerical results for Fe and Ni taking into account the dynamical corrections up to the second order [5]. In this presentation, we extend the calculations up to the 4th order, and demonstrate that the theory explains the finite-temperature properties of transition metals quantitatively or semiquantitatively.

The dynamical CPA is a dynamical version of the single-site spin fluctuation theory developed by Cyrot, Hubbard, and Hasegawa since early in the 1970, and has recently been shown to be equivalent to the dynamical mean field theory (DMFT) [1, 6]. The theory describes the magnetic properties at finite temperatures efficiently taking into account the dynamical corrections to the static approximation which is exact in the high temperature limit. Moreover the present approach can treat the transverse spin fluctuations for arbitrary d electron number, which is different from the early quantum Monte-Carlo (QMC) calculations combined with the DMFT [7].

¹ to be published in J. Phys.: Conference Series.

We adopted the Hamiltonian $H = H_0 + H_1$. The TB-LMTO Hamiltonian H_0 is written as

$$H_0 = \sum_{iL\sigma} \epsilon_{iL}^0 \hat{n}_{iL\sigma} + \sum_{iLjL'\sigma} t_{iLjL'} a_{iL\sigma}^\dagger a_{jL'\sigma}, \quad (1)$$

Here ϵ_{iL}^0 is an atomic level on site i and orbital L , $t_{iLjL'}$ is a transfer integral between orbitals iL and jL' . $L = (l, m)$ takes s , p , and d orbitals. $a_{iL\sigma}^\dagger$ ($a_{iL\sigma}$) is the creation (annihilation) operator for an electron with orbital L and spin σ on site i , and $\hat{n}_{iL\sigma} = a_{iL\sigma}^\dagger a_{iL\sigma}$ is a charge density operator for electrons with orbital L and spin σ on site i . It should be noted that ϵ_{iL}^0 is not identical with the atomic level ϵ_{iL} in the DFT-LDA potential because the latter contains exchange correlation contributions. For the atomic d level, we adopted the formula $\epsilon_{iL}^0 = \epsilon_{iL} - \partial E_{\text{LDA}}^U / \partial n_{iL\sigma}$ [4]. Here $n_{iL\sigma}$ is the charge density at the ground state, E_{LDA}^U is a LDA functional to the intraatomic Coulomb interactions. We adopted the Hartree-Fock type form for E_{LDA}^U proposed by Anisimov *et al.* [8] because we treat here the itinerant electron system where the ratio of the Coulomb interaction to the d band width is not larger than one. For the other orbital electrons, we did not make any corrections for simplicity.

The intraatomic Coulomb interactions H_1 is given as

$$H_1 = \sum_i \left[\sum_m U_0 \hat{n}_{ilm\uparrow} \hat{n}_{ilm\downarrow} + \sum_{m>m'} (U_1 - \frac{1}{2}J) \hat{n}_{ilm} \hat{n}_{ilm'} - \sum_{m>m'} J \hat{\mathbf{s}}_{ilm} \cdot \hat{\mathbf{s}}_{ilm'} \right]. \quad (2)$$

Here U_0 (U_1) and J in the interaction H_1 are the intra-orbital (inter-orbital) Coulomb interaction and the exchange interaction, respectively. \hat{n}_{ilm} ($\hat{\mathbf{s}}_{ilm}$) with $l = 2$ is the charge (spin) density operator for d electrons on site i and orbital m .

We have presented the first-principles dynamical CPA in our previous paper [5]. We briefly explain here the outline. In the theory, we transform the interacting Hamiltonian H_1 into a dynamical potential v in the free energy adopting the functional integral method. Introducing a uniform medium, (*i.e.* a coherent potential) $\Sigma_{L\sigma}(i\omega_n)$, we expand the free energy with respect to sites. Note that ω_n denotes the Matsubara frequency. The first term in the expansion is the free energy for a uniform medium, $\tilde{\mathcal{F}}[\Sigma]$. The second term is an impurity contribution to the free energy. The dynamical CPA neglects the higher-order terms, so that the free energy per atom is given by

$$\mathcal{F}_{\text{CPA}} = \tilde{\mathcal{F}}[\Sigma] - \beta^{-1} \ln C \int d\xi e^{-\beta E_{\text{eff}}(\xi)}. \quad (3)$$

Here β is the inverse temperature. C is a normalization constant. ξ is the static field variable on a site. $E_{\text{eff}}(\xi)$ is an effective potential projected onto the static field ξ . It consists of the static contribution $E_{\text{st}}(\xi)$ and the dynamical correction term $E_{\text{dyn}}(\xi)$. We obtain the latter using the harmonic approximation (see Ref. [5] for details of expressions of $E_{\text{st}}(\xi)$ and $E_{\text{dyn}}(\xi)$).

The effective medium, *i.e.*, the coherent potential can be determined by the stationary condition $\delta \mathcal{F}_{\text{CPA}} / \delta \Sigma = 0$. This yields the CPA equation as

$$\langle G_{L\sigma}(\xi, i\omega_l) \rangle = F_{L\sigma}(i\omega_l). \quad (4)$$

Note that $\langle \rangle$ at the r.h.s. is a classical average taken with respect to the effective potential $E_{\text{eff}}(\xi)$, $F_{L\sigma}(i\omega_l) = [(i\omega_l - \mathbf{H}_0 - \Sigma)^{-1}]_{iL\sigma iL\sigma}$ is the coherent Green function, where $(\mathbf{H}_0)_{iL\sigma jL'\sigma}$ is the one-electron TB-LMTO Hamiltonian matrix, and $(\Sigma)_{iL\sigma jL'\sigma} = \Sigma_{L\sigma}(i\omega_l) \delta_{ij} \delta_{LL'}$. Furthermore, $G_{L\sigma}(\xi, i\omega_l)$ is the impurity Green function given by

$$G_{L\sigma}(\xi, i\omega_l) = \tilde{g}_{L\sigma\sigma}(i\omega_l) - \frac{\beta}{\kappa_{L\sigma}(i\omega_l)} \frac{\delta E_{\text{dyn}}(\xi)}{\delta \Sigma_{L\sigma}(i\omega_l)}. \quad (5)$$

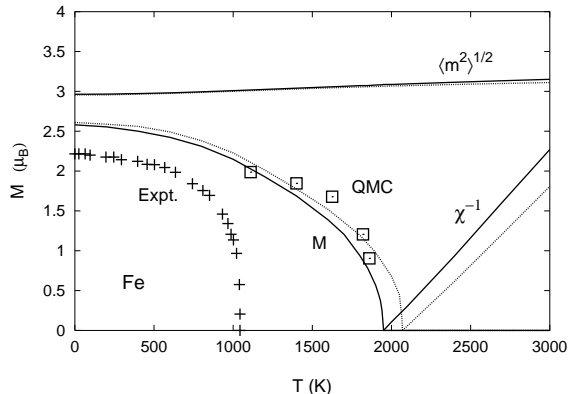


Figure 1. Magnetization (M), inverse susceptibility (χ^{-1}), and amplitude of local moment ($\langle \mathbf{m}^2 \rangle^{1/2}$) vs. temperature (T) curves for Fe. The dynamical results are shown by the solid curves, while the results in the static approximation are shown by dotted curves. The DMFT results without transverse spin fluctuations [7] are shown by open squares. Experimental data of magnetization [10] are shown by +.

Here the first term at the r.h.s. is the Green function in the static approximation. The second term is the dynamical corrections, and $\kappa_{L\sigma}(i\omega_l) = 1 - F_{L\sigma}(i\omega_l)^{-2} \delta F_{L\sigma}(i\omega_l) / \delta \Sigma_{L\sigma}(i\omega_l)$.

Solving the CPA equation (4) self-consistently, we obtain the effective medium. The magnetic moment is then given by $\langle \hat{m}_L^z \rangle = \beta^{-1} \sum_{n\sigma} \sigma F_{L\sigma}(i\omega_n)$, and the density of states (DOS) is obtained by means of a numerical analytic continuation.

In the numerical calculations, the average Coulomb and exchange energy parameters (\bar{U} and J) are taken from the LDA+U band calculations [4, 9]; $(\bar{U}, J) = (0.169, 0.066), (0.245, 0.069), (0.221, 0.066)$ Ry for Fe, Co, and Ni, respectively. U_0 and U_1 are obtained from the relations $U_0 = \bar{U} + 8J/5$ and $U_1 = \bar{U} - 2J/5$. These sets of parameters yield the Hartree-Fock Curie temperatures: 12200K, 12100K, and 4950K for Fe, Co, and Ni, respectively.

We present in Fig. 1 the results of calculations for Fe. The calculated susceptibility follows the Curie-Weiss law with the effective Bohr magneton number $m_{\text{eff}} = 3.0\mu_B$ in agreement with the experimental value $3.2\mu_B$. We find the Curie temperature $T_C = 2070\text{K}$ in the static approximation. By taking into account the dynamical corrections, the Curie temperature reduces to 1930 K, which is comparable to 1900K obtained by the QMC calculations of the DMFT without transverse exchange interaction. The theoretical T_C is higher than the experimental result 1043K by a factor of 1.8. The ground-state magnetization obtained by an extrapolation, $2.58 \mu_B$ is also considerably overestimated as compared with the experimental value $2.22 \mu_B$.

In the case of Ni, we obtained the Curie temperature $T_C = 1420\text{K}$ in the static approximation as shown in Fig. 2. The dynamical corrections much reduce the Curie temperature; $T_C = 620\text{K}$, which agrees well with the experimental value 630K. Calculated inverse susceptibility shows slightly upward convexity. We obtained the effective Bohr magneton number $m_{\text{eff}} = 1.6\mu_B$ in the high temperature region. The result agrees with the experimental one $1.6\mu_B$. As seen from Fig. 3, a large reduction of T_C in the dynamical CPA calculation seems to be related to the reduction of the DOS $\rho(0)$ at the Fermi level when we take into account the third and fourth order dynamical corrections. The behavior is consistent with the argument of the stability of ferromagnetism at the ground state [14].

We have also investigated the finite temperature magnetism for the fcc Co. In this case, we obtained $T_C = 2550\text{K}$ which is larger than the experimental value 1388K by a factor of 1.8. Calculated effective Bohr magneton number of Co is $3.0\mu_B$, being in good agreement with the experimental value $3.15\mu_B$. We have also calculated the densities of states from Sc to Cu in the high-temperature region, where the present theory works best, and found that the DOS explain well the XPS and BIS data. The correlation effects on these excitation spectra will be discussed in a separate paper.

In summary, we have presented the dynamical CPA combined with the first-principles

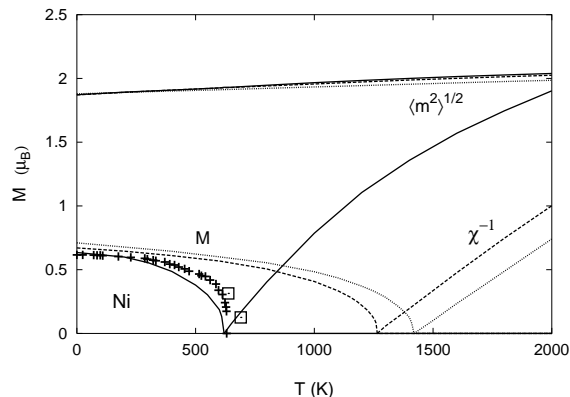


Figure 2. Magnetization, inverse susceptibility, and amplitude of local moment as a function of temperature for Ni. The dynamical results are shown by the solid curves, while the results in the static calculation are shown by dotted curves. Dashed curves show the results of the 2nd-order dynamical CPA. The DMFT results [7] are shown by open squares, and experimental data of magnetization [11] are shown by +.

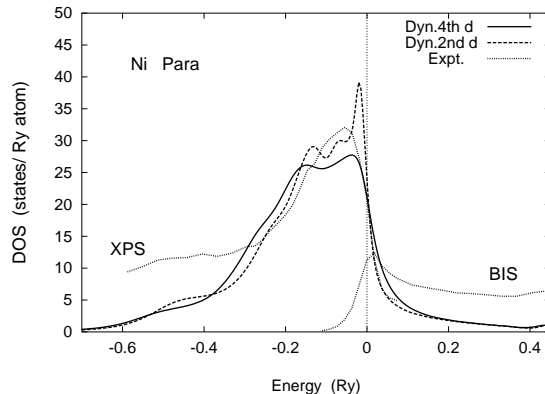


Figure 3. Calculated DOS in the paramagnetic Ni. Solid curve: dynamical CPA, dashed curve: 2nd-order dynamical CPA, dotted curves: XPS and BIS experimental data [12, 13].

TB-LMTO LDA+U Hamiltonian. Calculated Curie temperature T_C for Ni agrees with the experiment, but T_C for Fe and Co are higher than the experimental ones by a factor of 1.8. On the other hand, the present theory explains quantitatively the effective Bohr magneton numbers as well as the excitation spectra in the high temperature region. In order to obtain observed T_C , we have to take into account the nonlocal correlations definitely. Such an attempt is in progress.

This work was supported by Grant-in-Aid for Scientific Research (19540408). Numerical calculations were carried out with use of the Hitachi SR11000 in the Supercomputer Center, Institute of Solid State Physics, University of Tokyo.

References

- [1] Kakehashi Y 2004 Adv. in Phys. **53** 498
- [2] Kakehashi Y 1992 Phys. Rev. B **45** 7196; 2002 Phys. Rev. B **65** 184420
- [3] Andersen O K, Jepsen O, and Krier G 1994 in *Methods of Electronic Structure Calculations* ed. by V. Kumar, O.K. Andersen, and A. Mookerjee (World Scientific Pub., Singapore, 1994) p. 63
- [4] Anisimov V I, Aryasetiwan F, and Lichtenstein A I 1997 J. Phys. Condens. Matter **9** 767
- [5] Kakehashi Y, Shimabukuro T, Tamashiro T, and Nakamura T 2008 J. Phys. Soc. Jpn. **77** 094706
- [6] Kakehashi Y 2002 Phys. Rev. B **66** 104428
- [7] Lichtenstein A I, Katsnelson M I, and Kotliar G 2001 Phys. Rev. Lett. **87** 067205
- [8] V.I. Anisimov, I.V. Solovyev, and M.A. Korotin, M.T. Czyżyk, and G.A. Sawtzky: Phys. Rev. B **48** (1993) 16929.
- [9] Bandyopadhyay T and Sarma D D 1989 Phys. Rev. B **39** 3517; Mann J B 1967 Los Alamos Scientific Laboratory Rep. No. LASL-3690
- [10] Potter H H 1934 Proc. Roy. Soc. London A **146** S362
- [11] Weiss P and Forrer R 1926 Ann. Phys. Paris **5** S153
- [12] Narmonev A G and Zakharov 1988 Phys. Met. Metall. **65** 97
- [13] Speier W, Fuggle J C, Zeller R, Ackermann B, Szot K, Hillebrecht F U, and Campagna M 1984 Phys. Rev. B **30** 6921
- [14] Kanamori J 1963 Prog. Theor. Phys. **30** 275